ORIGINAL RESEARCH

# The functional curcumin liposomes induce apoptosis in C6 glioblastoma cells and C6 glioblastoma stem cells in vitro and in animals

Yahua Wang
Xue Ying
Haolun Xu
Helu Yan
Xia Li
Hui Tang

Key Laboratory of Xinjiang Phytomedicine Resources and Modernization of TCM, School of Pharmaceutical Sciences, Shihezi University, Shihezi, Xinjiang, People's Republic of China

**Abstract:** Glioblastoma is a kind of malignant gliomas that is almost impossible to cure due to the poor drug transportation across the blood–brain barrier and the existence of glioma stem cells. We prepared a new kind of targeted liposomes in order to improve the drug delivery system onto the glioma cells and induce the apoptosis of glioma stem cells afterward. In this experiment, curcumin was chosen to kill gliomas, while quinacrine was used to induce apoptosis of the glioma stem cells. Also, $p$-aminophenyl-α-D-mannopyranoside could facilitate the transport of liposomes across the blood–brain barrier and finally target the brain glioma cells. The cell experiments in vitro indicated that the targeted liposomes could significantly improve the anti-tumor effects of the drugs, while enhancing the uptake effects, apoptosis effects, and endocytic effects of C6 glioma cells and C6 glioma stem cells. Given the animal experiments in vivo, we discovered that the targeted liposomes could obviously increase the survival period of brain glioma-bearing mice and inhibit the growth of gliomas. In summary, curcumin and quinacrine liposomes modified with $p$-aminophenyl-α-D-mannopyranoside is a potential preparation to treat brain glioma cells and brain glioma stem cells.

**Keywords:** C6 glioblastoma stem cells, apoptosis, blood–brain barrier, curcumin liposomes, brain glioma-bearing rats

## Introduction

Glioblastoma multiforme (World Health Organization grade IV glioma or grade IV astrocytoma), the most common type of primary brain cancer, is associated with its resistance to conventional therapy and poor patient survival. It is also the most aggressive and lethal multiforme. Given the diagnosis, the median survival time is approximately 14 months even with intensive treatment, and less than 5% of patients survive beyond the third year.[1–3]

Chemotherapy failure is due to the inability to transport anticancer drugs to the brain tissues. An endothelial cell monolayer associated with pericytes and astrocytes, known as the blood–brain barrier (BBB), plays an important role in controlling the access of substances to the brain.[4] The BBB acts as a selective barrier and prevents toxic substances from passing through to the central nervous system (CNS). Small lipophilic molecules can be transported through the BBB freely by diffusion. Hydrophilic molecules, such as peptides and proteins, may enter the brain by specific transport mechanisms.[5] Transit limitation, as one of the characteristics of BBB, would lead to low amount of drug accumulation, which represents the most important barrier that must be overcome in the drug delivery to the CNS. In the current situation of emerging

Correspondence: Xue Ying
Department of Pharmacy, School of Pharmaceutical Sciences, Shihezi University, North 2nd Road, Shihezi 832000, People's Republic of China
Tel +86 135 7945 5890
Fax +86 099 3205 7939
Email yingxueshzu@163.com

neurologic diseases, transporting CNS drugs through the BBB remains a challenge in the research on CNS-targeted drugs. Also, vehicles for crossing the BBB are still in infancy and require a long run before full application.[6]

The current standard of treatment is not highly effective, which results in patients with tumor recurrence rarely surviving over 2 years. This might be attributed to the chemotherapy and radiation resistance in glioma stem cells (GSCs).[7,8] The discovery of highly tumorigenic GSCs, which comprise a self-renewing subpopulation of GSCs, suggested that therapeutic approaches to effectively eradicate these cells may improve patient outcome.[9] Furthermore, present studies have demonstrated[10–12] that chemotherapy only destroys the most bulky cancer cells but cannot eradicate cancer stem cells (CSCs). The existence of CSCs leads to chemoresistance and tumor recurrence. Therefore, eradicating the GSCs may represent an effective chemotherapeutic strategy, which thereby overcomes glioma recurrence.

Mannose receptors are transmembrane glycoproteins, which mainly express on the macrophages. These receptors specifically bind to mannosylated molecules and mediate their endocytosis. Ligand specificity and cellular distribution provide the mannose receptor with a highly important role in homeostasis and immune response. Recent researches have proved the expression of mannose receptors in the brain. Mannose receptors express on two main sites which are astrocytes and microglia.[13] Both of them could be derived to immune-competent cells. It is demonstrated that the delivery of glucose and glucose-like substances is mediated by a family of glucose carriers while crossing the BBB, such as 2-deoxyglucose, galactose, mannose, and glucose analogs.[5,14] Glucose transporter 1 (GLUT1), an isoform of GLUT, is primarily expressed at the luminal surface of the brain capillaries and the choroid plexus.[15] In a way, GLUT1 potentially enhances the delivery through BBB.[16] *p*-Aminophenyl-α-D-mannopyranoside (MAN), a kind of mannose analog, was modified on the surface of liposomes in the present study.[17] It was demonstrated that liposomes modified with MAN not only promote the penetration through the BBB into the brain, but also target the selected intracerebral regions, including the cortex, cerebellum, brainstem, hippocampus, and pontine nuclei.[18]

Curcumin is a kind of dietary polyphenol derived from the rhizomes of turmeric (*Curcuma longa*), which is usually used in the preparation of mustard and curry.[19] The anticancer effect of curcumin has been shown in many studies on cells and animals. Recent research has revealed that curcumin can target the CSCs. CSCs are proposed to be responsible for initiating and maintaining cancer.[20] They also contribute to the recurrence and drug resistance. In the past few years, numerous studies have suggested that curcumin holds the potential for targeting the CSCs in a direct or indirect way based on CSC self-renewal pathways.[21] Recent studies have revealed the effects of curcumin on the C6 glioma cell line from rat. The literature shows a decreased side population (SP) of C6 glioma cells after daily treatment with curcumin.[22]

Quinacrine has been used as an antiprotozoal, antirheumatic, and intrapleural sclerosing agent. It has also been used to induce cancer apoptosis through the mitochondrial pathway.[23] As a chemosensitizer, quinacrine is able to enhance the apoptosis effects on cancer cells that are induced by chemotherapeutic agents. The activation of p53 pathway and the suppression of PI3K/AKT/mTOR and NF-κB pathways all play key roles in the anticancer activity of quinacrine.[24–26]

Liposome, a drug delivery system for cancer therapy, is used for treating the tumors effectively with minimal side effects. Furthermore, it could also improve the drug stability and water solubility, while enhancing the drug's permeability and antitumor activity. In the present study, we constructed a targeted liposome (curcumin and quinacrine liposome modified with MAN) to eliminate glioblastoma and GSCs. MAN was used to indirectly transport curcumin and quinacrine acrossing the BBB. Quinacrine was used to enhance the apoptosis effects of curcumin. Both substances were projected to kill the glioma cells and GSCs.

# Materials and methods
## Preparation of different liposomes
To prepare different kinds of liposomes, curcumin (Xi'an Rongsheng Biological Technology Co., Ltd., Xi'an, People's Republic of China) and quinacrine (Shanghai Yuanye Biological Technology Co., Ltd., Shanghai, People's Republic of China) liposomes modified with MAN were prepared as targeted liposomes. Other kinds of liposomes were also prepared as controls. These liposomes included curcumin liposomes, curcumin and quinacrine liposomes, and curcumin and quinacrine liposomes modified with MAN.

### Preparation of curcumin liposomes
Curcumin liposomes were prepared using the method of film dispersion-pH gradient. Egg phosphatidylcholine (Germany Lipoid Company, Shanghai, People's Republic of China), cholesterol (CHOL; Beijing Shuangxuan Microbe Culture Medium Products Factory, Beijing, People's Republic of China), polyethylene glycol distearoylphosphophosphatidylethanolamine (PEG$_{2000}$-DSPE; NOF Corporation, Tokyo, Japan),

and 1,2-distearoyl-*sn*-glycero-3-phosphoethanolamine-N-[amino(polyethylene glycol) 2000] ($NH_2$-$PEG_{2000}$-DSPE; Avanti Polar Lipids, Alabaster, AL, USA) were mixed at a molar ratio of 65:30:4.5:0.5 (mmol/mmol) and dissolved in methanol in an eggplant-type flask. Then, curcumin was added to the eggplant-type flask (curcumin:phospholipids =1:40, w/w). Methanol was vaporized with a rotary vacuum evaporator (EYELA-1000S; EYELA Rikakikai Corporation, Tokyo, Japan) at 45°C, and then the lipid film was hydrated with ammonium sulfate (250 mM) for 5 min with an ultrasound bath. Subsequently, the suspensions were handled with ultrasonic cell disruptor (JY92 cell sonicator; Ningbo Chibio-Technology Co., Ltd., Ningbo, People's Republic of China) for 10 min. The suspensions were successively extruded through 400 and 200 nm pore size polycarbonate membranes (EMD Millipore, Billerica, MA, USA). After that, the suspensions were further dialyzed (cut-off molecular weight: 12,000–14,000) in phosphate-buffered saline (PBS; 137 mM NaCl, 2.7 mM KCl, 8 mM $Na_2HPO_4$, and 2 mM $KH_2PO_4$ at pH 7.4) for every 12 h. After dialyzing for three times, curcumin liposomes were obtained.

## Preparation of curcumin and quinacrine liposomes

The curcumin and quinacrine liposomes were prepared using the curcumin liposomes. The procedure is as follows. First, the curcumin liposomes were passed over a chromatographic separation column (Sephadex G-50 column; Sigma-Aldrich Co., Beijing local agent, People's Republic of China) in order to remove free curcumin. Then, the obtained suspensions were mixed with a certain amount of quinacrine dihydrochloride (quinacrine dihydrochloride:phospholipids =1:48, w/w). After this, the suspensions were incubated at 60°C in a water bath and gently shaken for 20 min to obtain curcumin and quinacrine liposomes. The obtained curcumin and quinacrine liposomes were dialyzed in PBS to remove the unencapsulated quinacrine.

## Preparation of curcumin and quinacrine liposomes modified with MAN

Curcumin and quinacrine liposomes modified with MAN (Sigma-Aldrich Co.) were prepared as targeted liposomes using the curcumin liposomes. The preparation methods for the liposomes modified with MAN were reported previously.[17] In brief, MAN was added to the curcumin liposome. An excessive amount of glutaraldehyde was slowly added to the liposomes; then, the suspensions were incubated for 5 min at room temperature. After this, uncoupled MAN and glutaraldehyde were removed by dialysis performed three times against PBS for every 8 h. As mentioned above, quinacrine was loaded to the curcumin liposomes modified with MAN to obtain the curcumin and quinacrine liposomes modified with MAN.

To evaluate the coupling efficiency of MAN, the uncoupled $NH_2$ group of $NH_2$-$PEG_{2000}$-DSPE on the liposomes modified with MAN was measured by spectrophotometry after adding trinitrobenzene sulfonic acid (Biodee Biotechnology Co., Ltd., Beijing, People's Republic of China) as a visualization reagent, which was described previously.[17,27] The absorbance of the final solution was estimated with an ultraviolet spectrophotometer (UV-2401PC; Shimadzu Technologies Inc., Cotati, CA, USA) at 320 nm containing a blank group of distilled water. The coupling efficiency of MAN on the liposomes was estimated with the formula $CE_{MAN} = (1 - A_{uncoupled}/A_{total}) \times 100\%$, where $CE_{MAN}$ is the coupling efficiency of MAN, $A_{uncoupled}$ is the absorbance of the uncoupled amino groups of $NH_2$-$PEG_{2000}$-DSPE on the targeted liposomes, and $A_{total}$ is the absorbance of the amino groups of $NH_2$-$PEG_{2000}$-DSPE before being conjugated with MAN.

# Characterization of different liposomes
## Encapsulation efficiency (EE)

The concentrations of curcumin and quinacrine in the liposomes were determined by a high-performance liquid chromatography (HPLC; Agilent Technologies Inc., Cotati, CA, USA) system with an octadecylsilyl-SP column (250×4.6 mm, 5 μm). The EEs of curcumin and quinacrine were calculated with the formula $EE = (W_{dialysis}/W_{total}) \times 100\%$, where EE is the encapsulation efficiency of curcumin or quinacrine, $W_{dialysis}$ is the measured amount of curcumin or quinacrine in the liposome suspensions after being dialyzed in PBS, and $W_{total}$ is the measured amount of curcumin or quinacrine in the initial liposome suspensions.

## Drug release

In vitro release of curcumin and quinacrine liposomes was performed by dialysis against the release medium (PBS containing 2% sodium dodecyl sulfate). The curcumin and quinacrine in the samples were measured by HPLC as described above, and the release rates of both drugs were estimated.

## Characterization of the liposomes

The particle size, polydisperisty indices, and zeta potential of liposomes were measured by light scattering particle size analyzer (Malvern Instruments, Malvern, UK). The shape and

surface morphology of the liposomes were then investigated by transmission electron microscopy (600×) or TEM (JEM-ARM200F; JEOL, Tokyo, Japan) after negative staining with uranyl acetate solution (1%, w/v).

## Cell culture

### Culture of C6 glioblastoma cells

C6 glioblastoma cells (Institute of Sciences, Shanghai, People's Republic of China) were grown in Dulbecco's Modified Eagle's Medium (DMEM, high glucose; Gibco Biotech Co., Ltd., Beijing local agent, People's Republic of China) supplemented with 10% heat-inactivated fetal bovine serum (Hangzhou Evergreen Company, Hangzhou, People's Republic of China), 100 U/mL of penicillin, and 100 µg/mL of streptomycin (Gibco Biotech Co., Ltd.), maintained in a humidified atmosphere at 37°C with 5% $CO_2$.

### Culture and identification of GSCs

After being dissociated by 0.25% trypsin (Gibco Biotech Co., Ltd.), C6 glioblastoma cells were plated in serum-free DMEM-F12 (Macgene Gen Techology Co., Ltd., Beijing, People's Republic of China) supplemented with 10 ng/mL basic fibroblast growth factor (Macgene Gen Techology Co., Ltd.), 20 ng/mL epidermal growth factor (Macgene Gen Techology Co., Ltd.), and 2% B27 (Gibco Biotech Co., Ltd.). Under these conditions, the C6 GSCs grew as nonadherent spherical clusters of cells. Half of the medium was changed every other day. After 5 days, the GSC spheres were collected by centrifugation at 1,000 rpm for 5 min and cultured in the serum-free medium under 5% $CO_2$ at 37°C.

To identify the GSCs, the collected GSC spheres, which were enzymatically dissociated and washed in PBS, were gathered after 3 weeks. The samples were fixed with 4% paraformaldehyde as a fixative for 10 min. After being penetrated with a 0.1% saponin-balanced salt solution for permeabilization, the cells were incubated with monoclonal anti-mouse/rat nestin phycoerythrin and their appropriate isotype controls (R&D Systems, Minneapolis, MN, USA) for 30 min in the dark. Afterward, the samples were washed thrice and resuspended in 500 µL cold PBS. Then, a FACScan flow cytometry (Becton Dickinson FACSCalibur, Mountain View, CA, USA) was performed.[28,29]

## Cytotoxic analysis of C6 glioblastoma cells and GSCs

C6 glioblastoma cells and GSCs were seeded in 96-well plates at a density of $8 \times 10^3$ cells/well and subsequently incubated in serum-containing culture medium at 37°C under 5% $CO_2$. Free quinacrine, free curcumin, free curcumin plus quinacrine, curcumin liposomes, curcumin and quinacrine liposomes, and curcumin and quinacrine liposomes modified with MAN were added to the 96-well plates. The culture medium was used as blank control. The final concentrations of curcumin in the experimental groups were 0.05, 0.1, 0.25, 1, 2.5, 5, 7, and 10 µM, separately. After treatment for 48 h, a cytotoxicity assay was performed by sulforhodamine B (Sigma, Cotati, CA, USA) staining assay. The absorbance at 540 nm was detected with a microplate reader (BIO-RAD Model 680; Bio-Rad Laboratories, Inc., Shanghai, People's Republic of China). Inhibitory rate was calculated by the formula inhibitory rate (%) = 1 − ($A_{540 \ nm}$ for the treated cells/$A_{540 \ nm}$ for the control cells) ×100%, where $A_{540 \ nm}$ is the absorbance value.

## Ability of inducing apoptosis in C6 glioblastoma cells and GSCs

Apoptosis was detected using a fluorescein isothiocyanate Annexin V staining kit by FACScan flow cytometer. In brief, C6 glioma cells and GSCs were seeded into six-well plates at a density of $5 \times 10^5$ cells/well and then incubated in serum-containing culture medium at 37°C with 5% $CO_2$. The cells were treated with free curcumin, free curcumin plus quinacrine, curcumin liposomes, curcumin and quinacrine liposomes, and curcumin and quinacrine liposomes modified with MAN for 24 h, respectively. The final concentration of curcumin was 8 µM. After incubation, the cells were assessed by flow cytometry in accordance with the manufacturer's instructions.

## C6 glioma stem cellular uptake

For visually estimating the uptake effects by C6 GSCs, laser scanning confocal microscope (LSM 510; Carl Zeiss Meditec AG, Jena, Germany) was used to observe the intracellular localization of liposome formulations in C6 GSCs.[30] C6 GSCs were seeded into 12-well plates at a density of $5 \times 10^3$ cells/well and incubated in serum-containing culture medium at 37°C. Then, the cells were treated with free curcumin, free curcumin plus quinacrine, curcumin liposomes, curcumin and quinacrine liposomes, and curcumin and quinacrine liposomes modified with MAN for 2 h. Curcumin was added to the cells at a final concentration of 8 µM. After washing the cells twice with PBS, they were fixed with 4% (v/v) paraformaldehyde and finally stained with Hoechst 33258 (Sigma-Aldrich Co.). The microscopic images of intracellular localization were obtained by laser scanning confocal microscope with an excitation wavelength

of 488 nm and an absorption wavelength of 550 nm. Data were analyzed through Aim Image Examiner.

The C6 glioma cells and C6 GSCs were seeded into six-well plates at a density of $2\times10^5$ cells/well and incubated in serum-containing culture medium at 37°C. The cells were then treated with different curcumin formulations and incubated at 37°C for 2 h. The formulations included free curcumin, free curcumin plus quinacrine, curcumin liposomes, curcumin and quinacrine liposomes, and curcumin and quinacrine liposomes modified with MAN. Then, the cells were trypsinized and collected by centrifugation (1,000 rpm, 5 min) after being washed twice with PBS. The fluorescence intensities of the cells were determined by FACScan flow cytometer.

## Ability of crossing the BBB monolayer and targeting GSCs

### Culture of mouse brain microvascular endothelial cells (bEnd.3 cells)

The BBB model was established using a method described previously.[17,31] bEnd.3 cells (Biaowu Procell Biotechnology Co., Ltd., Beijing, People's Republic of China) were cultured in the endothelial cell culture medium at 37°C with 5% $CO_2$. The culture medium consisted of DMEM (high glucose; Gibco Biotech Co., Ltd.), 20% fetal calf serum (high glucose; Gibco Biotech Co., Ltd.), 100 U/mL penicillin, and 100 mg/mL streptomycin.

### Simulation of BBB in vitro

The BBB model was used in vitro to investigate the BBB transcytosis property of liposomes. Briefly, the bEnd.3 cells were seeded in the apical chamber of transwells (Corning Co., Ltd., NY, USA; 0.4 µm pore size, 12 mm diameter, and 1.12 cm$^2$ surface area) at a density of $2\times10^4$ cells/well and incubated at 37°C. The culture medium was changed every 2 days. The tightness of the BBB model in vitro was detected by measuring the transendothelial electrical resistance (TEER) value. The BBB model was used for further experiments if the TEER value was higher than 150 Ω·cm$^2$.

### Transport across the BBB model in vitro

To evaluate the transport ratio of curcumin across the BBB, varying drug formulations were added to the transwells, including free curcumin, free curcumin plus quinacrine, curcumin liposomes, curcumin and quinacrine liposomes, and curcumin and quinacrine liposomes modified with MAN. The final concentration of curcumin was 8 µM. After treatment, a volume of 500 µL sample was taken from the basal chamber at 2, 4, 8, and 24 h. The concentration of curcumin was measured by HPLC as above. After each sampling, a volume of 500 µL of fresh serum-free DMEM was added to the basal chamber. The transport ratio of curcumin was then calculated with the formula: ratio% = $(C_n/C_{total})\times100\%$, where $C_n$ is the concentration of curcumin in the basal chamber at different hours and $C_{total}$ is the concentration of curcumin added in the apical chamber.

### Evaluations in the co-cultured model in vitro

To evaluate the inhibitory effects of C6 glioma cells and C6 GSCs after they were treated with different curcumin formulations, the BBB model was incubated in transwell inserts and then transferred to 12-well culture plates where C6 glioma cells and C6 GSCs were cultured.[32] The co-cultured model was established in the transwell chambers of two kinds of cells in vitro. Then, different curcumin formulations were applied to the apical chamber of these transwells, including free curcumin, free curcumin plus quinacrine, curcumin liposomes, curcumin and quinacrine liposomes, and curcumin and quinacrine liposomes modified with MAN. The final concentration of curcumin was 8 µM. After being incubated for 2 h, the inserts were moved away and GSCs were further incubated for 48 h. Subsequent procedures were the same as those used in the sulforhodamine B assay.

## Construction and evaluation of animal models in vivo

Imprinting control region (ICR) male mice weighing 18–20 g were purchased from Xinjiang Medical University (Xinjiang, People's Republic of China). The animals were housed under standard conditions with free access to food and water. All the experimental protocols were performed in accordance with the national guidelines of the principles for care and use of laboratory animals and were approved by the Institutional Animal Care and Use Committee of Shihezi University.

### Construction of animal models

ICR mice bearing GSCs were prepared as reported previously.[29,32] The mice were then separately made to settle on the brain stereotaxic apparatus after anesthetizing them with urethane at a dosage of 1 g/kg. The skin on the right forehead was prepared and sterilized with 75% ethanol. A vertical incision was made on the scalp along the bregma (the junction of the coronal and sagittal sutures) and the skull was exposed. The skull was then drilled 0.4 mm at the front of the coronal suture as well as 2 mm at the right of the sagittal suture. The tip of the needle was vertically and slowly

inserted 3.0 mm beneath the endocranium along the hole and 1 μL stem cell suspension ($5\times10^4$ cells/μL) was gradually injected every minute with the total amount being 3 μL if the needle was settled. The needle was removed 1 min after the injection, which was followed by closing the hole with bone wax. The incision was stitched, the skin sterilized, and penicillin was injected intramuscularly.

## Determination of growth curves

The animals were treated with drugs 10 days after the models had been successfully constructed. The animals were then randomly divided into six groups for growth curve determination. Curcumin group was treated with curcumin at a dose of 5 mg/kg injected through the tail vein. Physiological saline, free curcumin, free curcumin and quinacrine, curcumin liposomes, curcumin and quinacrine liposomes, and curcumin and quinacrine liposomes modified with MAN were administered every other day for four times. The survival rates were calculated with Statistical Package for the Social Sciences using Kaplan–Meier methods and the growth curves drawn.

## Tumor inhibitory rates

The animal models were treated with physiological saline, free curcumin, free curcumin and quinacrine, curcumin liposomes, curcumin and quinacrine liposomes, and curcumin and quinacrine liposomes modified with MAN for 10 days. At day 18, four mice from each group were anesthetized and the tumors were assessed through a coronal incision made along a puncture point on the brain surface. Then, we estimated the size of the tumor with the formula: tumor volume = $a^2 \times b \times \pi/6$, where a refers to the short diameter and b refers to the long diameter of the tumor. The tumor inhibitory rate was calculated by the formula: $Rv = V_{drug}/V_{saline} \times 100\%$, where $V_{saline}$ represents the average volume of the tumors in the physiological saline group and $V_{drug}$ represents the average volume of the tumors in the experimental groups.

## Hematoxylin–eosin (HE) staining

The treated animals were killed at day 18 after the models had been successfully built. The brain tissues were then made to settle in 4% paraformaldehyde. After that, the tissues were dehydrated by graded ethanol, decolorized by xylene, and embedded by dipping into wax. Finally, the brain blocks obtained from the tumor were cut into 6 μm thick slices along the coronal suture. Then, the sections were stained by HE and examined under light microscopy.

## Statistical analysis

Data are presented as the mean ± standard deviation (SD). One-way analysis of variance was used to determine the significance among groups, after which post hoc tests with the Bonferroni correction were used for comparison between individual groups. A $P$-value $<0.05$ was considered to be significant.

# Results
## Characterization of different liposomes

Table 1 lists the EE, modifying efficiency of MAN, and the particle size, polydispersity indices, and zeta potential of the curcumin and quinacrine liposomes modified with MAN. The results for the curcumin and quinacrine liposomes modified with MAN were: 94.32%±0.71%, 34.95%±0.15%, 119.7±0.17 nm, 0.22±0.01, and −2.73±0.74 mV, respectively. The liposomal EEs of curcumin and quinacrine were >80%.

Figure 1A shows a TEM image of curcumin and quinacrine liposomes modified with MAN. The curcumin and quinacrine liposomes modified with MAN were round shaped with a smooth surface and uniform particle size.

Figure 1B shows that the release rates of curcumin from the curcumin plus quinacrine liposomes, curcumin and quinacrine liposomes modified with MAN, and free curcumin plus quinacrine were 17.17%±0.04%, 20.14%±0.05%, and 52.12%±0.17%, respectively, at 48 h. Figure 1C shows

**Table 1** Characterization of different liposomes

| Formulations | Encapsulation efficiency (%) | | Modifying efficiency (%) | Particle size (nm) | PDI | Zeta potential (mV) |
|---|---|---|---|---|---|---|
| | Curcumin | Quinacrine | MAN | | | |
| Blank liposomes | – | – | – | 115.0±0.44 | 0.12±0.02 | −10.35±0.74 |
| Curcumin liposomes | 97.40±0.34 | – | – | 115.7±0.37 | 0.13±0.12 | −9.57±0.49 |
| Curcumin plus quinacrine liposomes | 95.33±0.85 | 94.13±0.49 | – | 117.4±0.44 | 0.13±0.01 | −8.56±0.22 |
| MAN-targeting curcumin plus quinacrine liposomes | 94.32±0.71 | 93.25±0.51 | 34.95±0.15 | 119.7±0.17 | 0.22±0.01 | −2.73±0.74 |

**Note:** Data are presented as the mean ± SD.
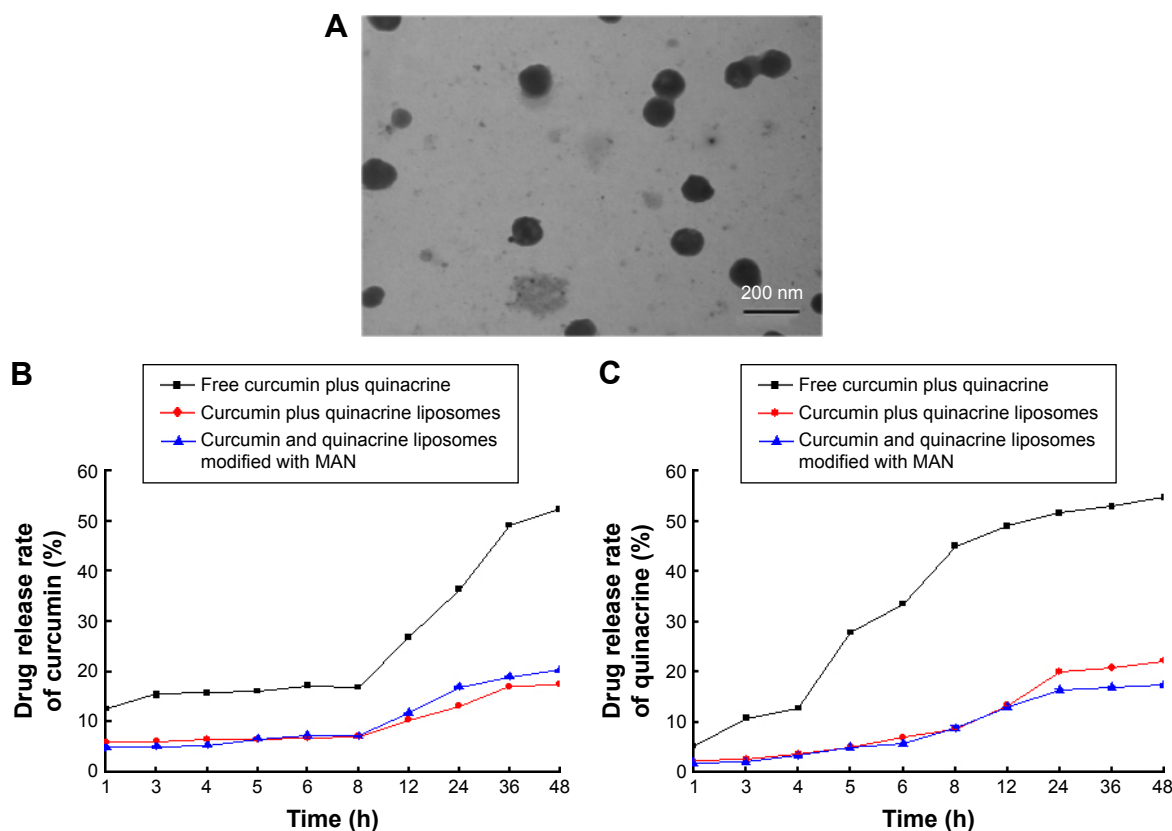**Abbreviations:** MAN, p-aminophenyl-α-D-mannopyranoside; PDI, polydisperisty indices; SD, standard deviation.

**Figure 1** Characterization of curcumin and quinacrine liposomes modified with MAN.
**Notes:** (**A**) TEM picture of curcumin and quinacrine liposomes modified with MAN. (**B**, **C**) Release rates of curcumin and quinacrine from three different formulations was determined by dialysis against PBS solution at 37°C, which contained 2% of SDS. Meanwhile, they were treated with a shaker using a frequency approximately 100 times per minute. Data are presented as the mean ± standard deviation, and each assay was repeated in triplicate.
**Abbreviations:** MAN, *p*-aminophenyl-α-D-mannopyranoside; PBS, phosphate-buffered saline; SDS, sodium dodecyl sulfate; TEM, transmission electron microscopy.

that the release rates of quinacrine from the curcumin plus quinacrine liposomes, curcumin and quinacrine liposomes modified with MAN, and free curcumin plus quinacrine were 21.97%±0.01%, 17.21%±0.32%, and 54.5%±0.54%, respectively, at 48 h.

## Cell culture and identification of GSCs

Figure 2A and B shows the images of C6 glioma cells and GSC spheroids, respectively. Figure 2C and D identifies the phenotypes of GSCs after being marked by nestin[+]. Results demonstrated that GSC spheres cultured in serum-free medium for 3 weeks displayed higher level of nestin (marked as nestin[+]). Figure 2C shows that purity of GSC dissociated from the C6 glioma cells in serum-contained medium was 19.84%. Figure 2D reveals that the purity of GSCs dissociated from the spheres in serum-free culture medium was 83.22% compared with isotype control. Nevertheless, C6 glioma cells cultured in serum-containing medium displayed lower level of nestin (marked as nestin[+]) compared with GSC spheres.

## Cytotoxic analysis of C6 glioblastoma cells and GSCs

Figure 3A and B illustrates the cytotoxic effects to C6 glioma cells and GSCs after they were treated with different formulations. Curcumin and quinacrine liposomes modified with MAN exhibited the strongest inhibitory effects on both glioma cells and GSCs. For curcumin and quinacrine liposomes modified with MAN (curcumin concentration was 8 µM), the cytotoxic effects to C6 glioma cells and GSCs were 96.52%±0.06% and 96.27%±0.34%, respectively, at 48 h.

## Apoptotic effects on C6 glioblastoma cells and GSCs

C6 glioblastoma cells and GSCs were stained with Annexin V-allophycocyanin 7-amino-actinomycin D in order to investigate whether the reduction in cell viability triggered by various formulations was associated with apoptosis. As shown in Figure 4A1–A5, early apoptotic populations of C6 glioblastoma cells induced by free curcumin, curcumin plus
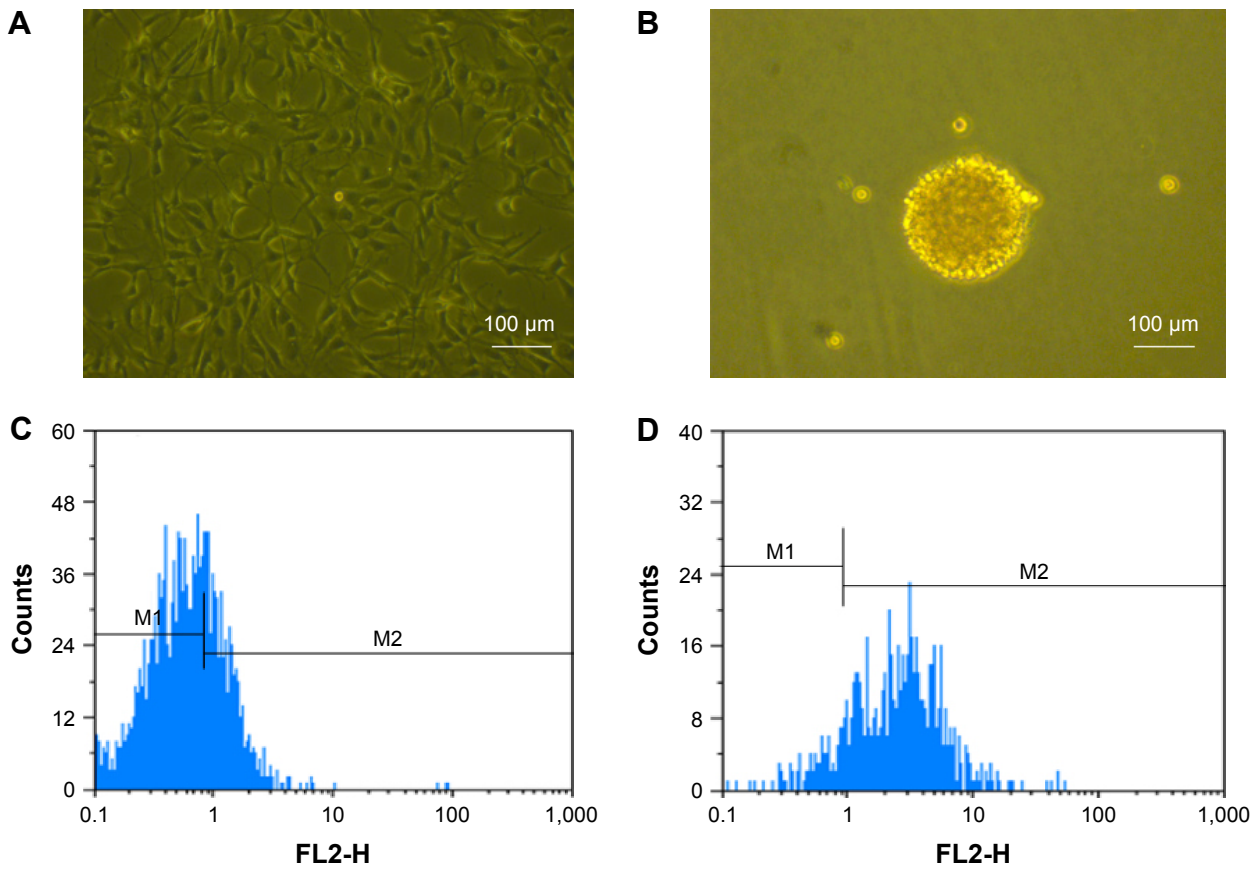
**Figure 2** Images of two kinds of cells.
**Notes:** (**A**) Images of C6 glioblastoma cells. (**B**) Images of GSCs. (**C**) C6 glioblastoma cells stained with anti-mouse/rat nestin phycoerythrin antibiodies. (**D**) GSC spheroids stained with anti-mouse/rat nestin phycoerythrin antibodies.
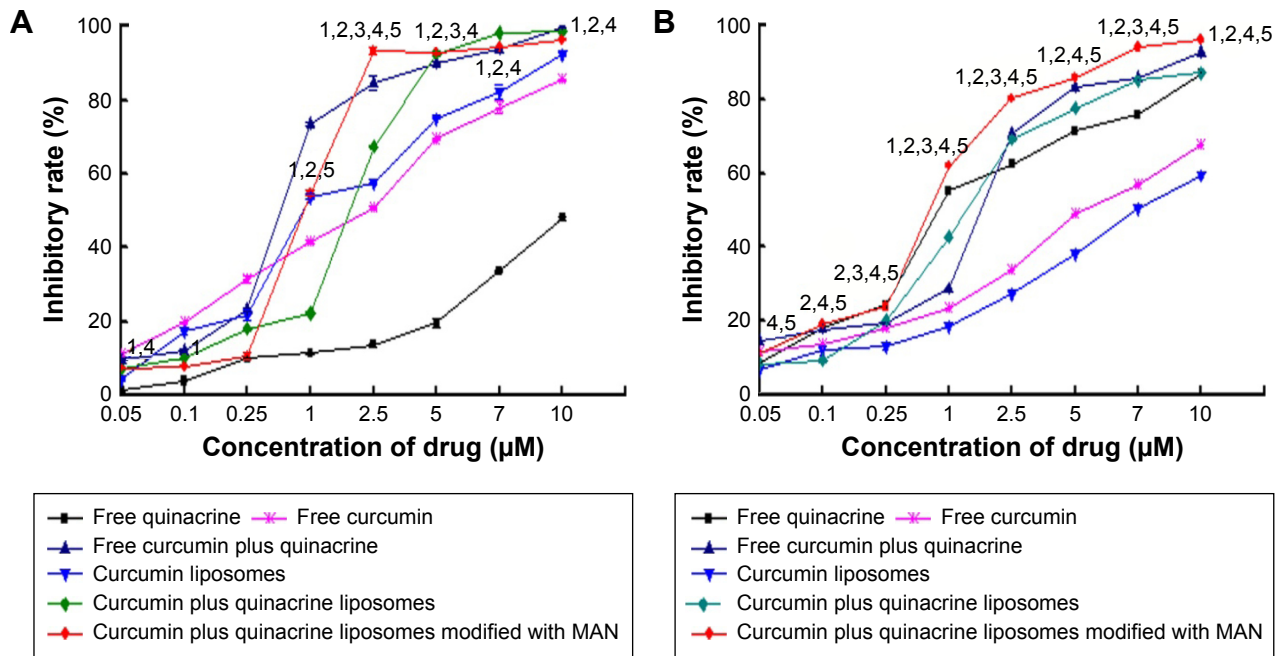**Abbreviations:** GSCs, glioma stem cells; FL2-H, FL2-height.



**Figure 3** The cytotoxic effects on cells after they were treated with varying formulations.
**Notes:** (**A**) The cytotoxic effects on C6 glioblastoma cells. (**B**) The cytotoxic effects on C6 glioblastoma stem cells. 1, $P<0.05$, versus free curcumin; 2, $P<0.05$, versus quinacrine; 3, $P<0.05$, versus free curcumin plus quinacrine; 4, $P<0.05$, versus curcumin liposomes; 5, $P<0.05$, versus curcumin and quinacrine liposomes.
**Abbreviation:** MAN, *p*-aminophenyl-α-D-mannopyranoside.

quinacrine, curcumin liposomes, curcumin and quinacrine liposomes, and curcumin and quinacrine liposomes modified with MAN were 6.28%±0.52%, 29.80%±1.76%, 53.40%±0.73%, 56.93%±1.82%, and 59.19%±1.34%, respectively. For C6 GSCs (Figure 4B1–B5), the apoptotic effects were induced by the formulations in the following order: curcumin and quinacrine liposomes modified with MAN (31.56%±1.34%) > curcumin and quinacrine liposomes (24.48%±0.57%) > curcumin liposomes (18.87%±1.35%) > free curcumin plus quinacrine (14.82%±0.50%) > free curcumin (10.01%±0.47%). Based on the results given above, Figure 4C was obtained by calculating the percentages of apoptotic population from three independent experiments, and showed the apoptosis capability which was induced by treating varing formulations with C6 glioblastoma cells and GSCs. Results presented in Figure 4C show that curcumin and quinacrine liposomes modified with MAN exhibited significant apoptotic effects on GSCs than other control groups.

## C6 glioma stem cellular uptake assay

In Figure 5A–E are observed the images obtained by laser scanning confocal microscopy showing all the drugs co-localized in the C6 GSCs 2 h after being directly treated with various formulations. Curcumin formulations were observed to penetrate into the nucleus and cytoplasm of the C6 GSCs (Figure 5A–E). Furthermore, a greater number of curcumin and quinacrine liposomes modified with MAN penetrated into the nucleus and cytoplasm than those of free curcumin, free curcumin plus quinacrine, curcumin liposomes, and curcumin and quinacrine liposomes. The drugs were mainly distributed in the nucleus of the C6 GSCs after endocytosis. Curcumin and quinacrine liposomes modified with MAN exhibited the fullest distribution in C6 GSCs.

Figure 5F shows the uptake assay of the C6 glioma cells and GSCs, as observed by flow cytometry. The uptake rates of C6 glioblastoma cells and GSCs were obtained after three independent experiments and the application of various formulations. The order of uptake rate of GSCs was: curcumin and quinacrine liposomes modified with MAN (93.70%±1.50%) > curcumin and quinacrine liposomes (86.41%±0.59%) > curcumin liposomes (83.40%±0.44%) > free curcumin plus quinacrine (78.67%±0.76%) > free curcumin (73.58%±0.89%).

## Ability for crossing BBB monolayer and GSC targeting

### Transport across the BBB model in vitro

The TEER value of the BBB model was >180 $\Omega \cdot cm^2$. Therefore, the BBB model was applied for further experiments. Curcumin and quinacrine liposomes modified with MAN exhibited the strongest transport effect than that of free curcumin, free curcumin plus quinacrine, curcumin liposomes, and curcumin
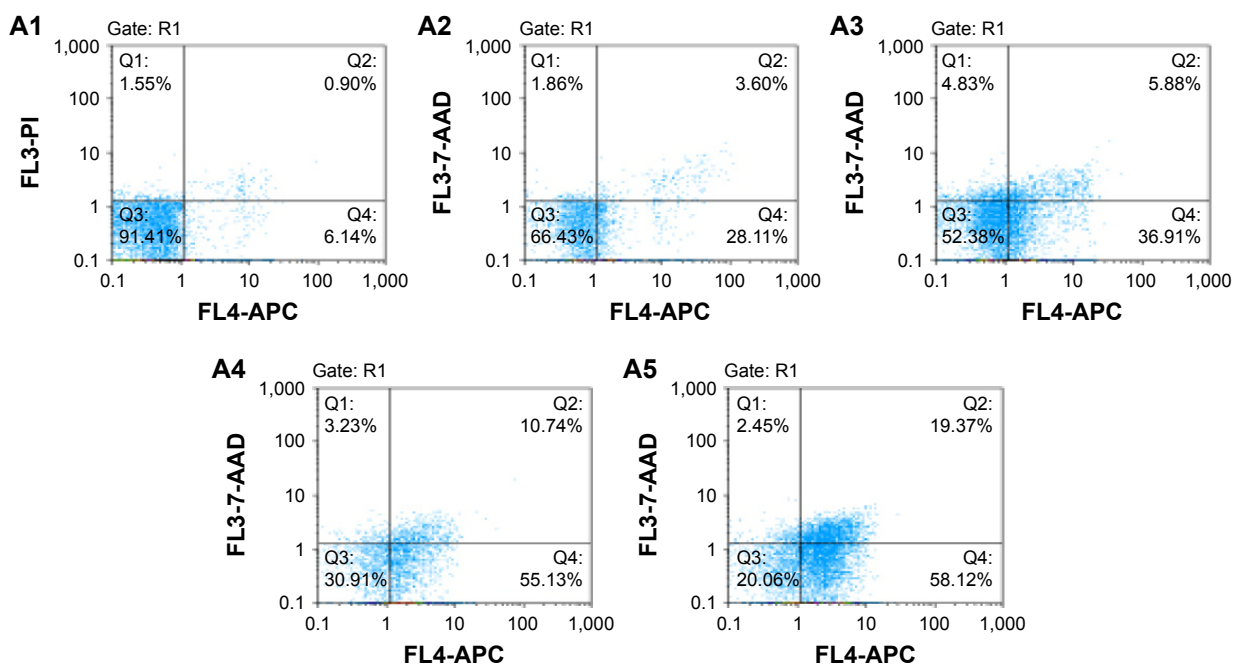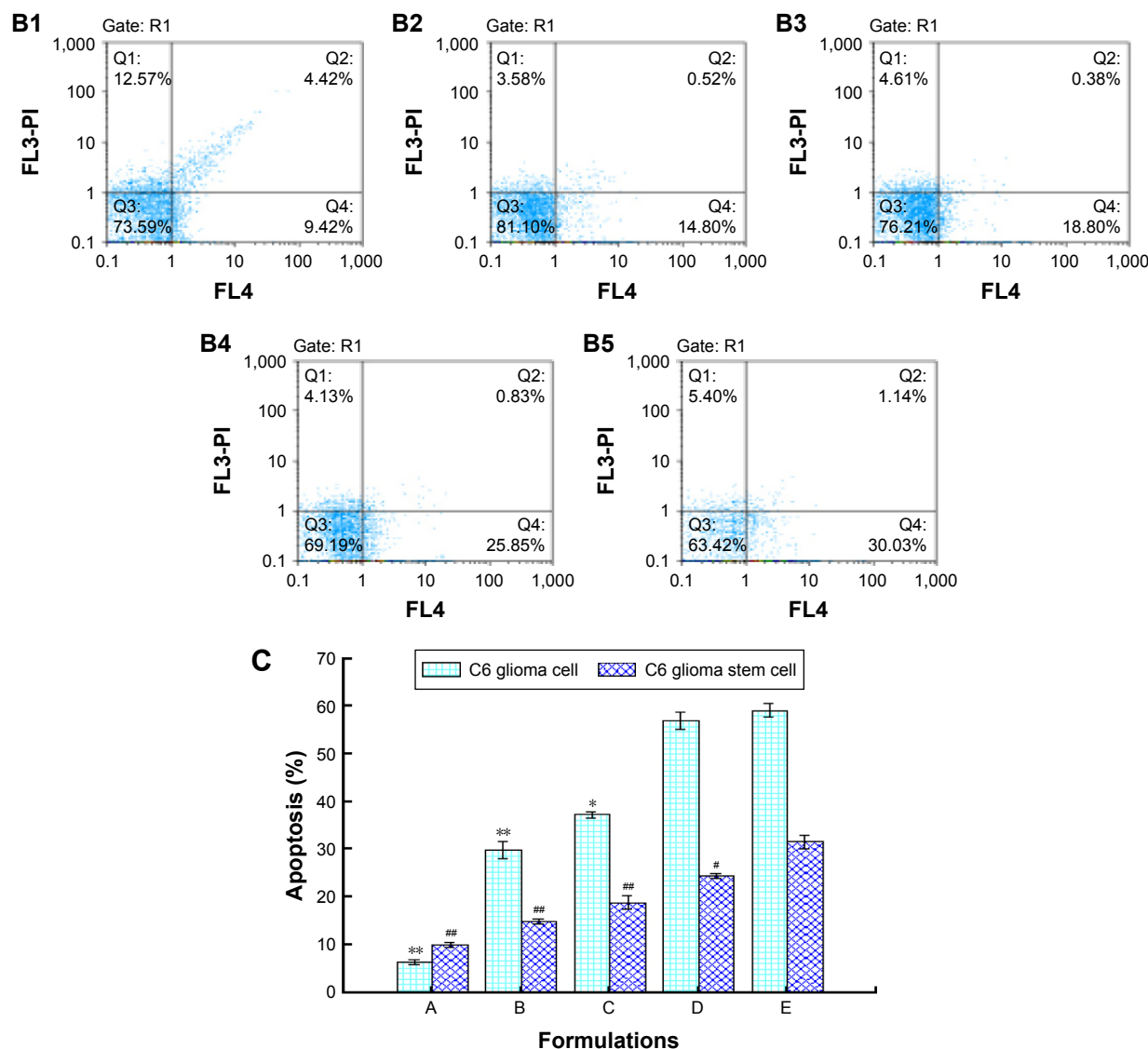


**Figure 4** (*Continued*)

**Figure 4** Apoptotic effects against C6 glioma cells and GSCs treated by varying fomulations.

**Notes:** Images (**A1–A5**) represent the apoptotic population on the basis of the results of the apoptosis assay in C6 glioma cells after they were treated with free curcumin, curcumin and quinacrine, curcumin liposomes, curcumin and quinacrine liposomes, and curcumin and quinacrine liposomes modified with MAN for 24 h. The assay was performed by flow cytometry analysis by staining with Annexin V-APC and 7-AAD. Images (**B1–B5**) represent the apoptotic population on the basis of the results of the apoptosis assay in GSCs after treatment with free curcumin, curcumin and quinacrine, curcumin liposomes, curcumin and quinacrine liposomes, and curcumin and quinacrine liposomes modified with MAN. (**C**) The figure was obtained by calculating the percentage of apoptotic population from three independent experiments on C6 glioblastoma cells and GSCs. Data are presented as the mean ± standard deviation. *$P$<0.05, versus curcumin and quinacrine liposomes modified with MAN in C6 glioma cells; **$P$<0.01, versus curcumin and quinacrine liposomes modified with MAN in C6 glioma cells; #$P$<0.05, versus curcumin and quinacrine liposomes modified with MAN in C6 glioma stem cells; ##$P$<0.01, versus curcumin and quinacrine liposomes modified with MAN in C6 glioma stem cells.

**Abbreviations:** GSCs, glioma stem cells; MAN, $p$-aminophenyl-α-D-mannopyranoside; Annexin V-APC, Annexin V-allophycocyanin; 7-AAD,7-amino-actinomycin D.

and quinacrine liposomes. All the groups were tested at different time points in a time-dependent manner (Figure 6A).

## Evaluations on the co-cultured model in vitro

To further understand the targeting effects, the inhibitory effects on the C6 glioma cells and GSCs were determined after the drug crossed through the BBB (Figure 6B). The inhibitory effects on the GSCs were in the following order: curcumin and quinacrine liposomes modified with MAN (59.05%±0.93%) > curcumin and quinacrine liposomes (24.73%±0.84%) > free curcumin plus quinacrine (12.07%±0.47%) > curcumin liposomes (11.52%±0.69%) > free curcumin (9.61%±0.37%). For the glioma cells, the order was: curcumin and quinacrine liposomes modified with MAN (55.24%±0.97%) > curcumin and quinacrine liposomes (23.74%±0.88%) > curcumin liposomes (18.63%±0.75%) > free curcumin plus quinacrine (15.73%±0.72%) > free curcumin (12.22%±0.67%). These results demonstrated that the
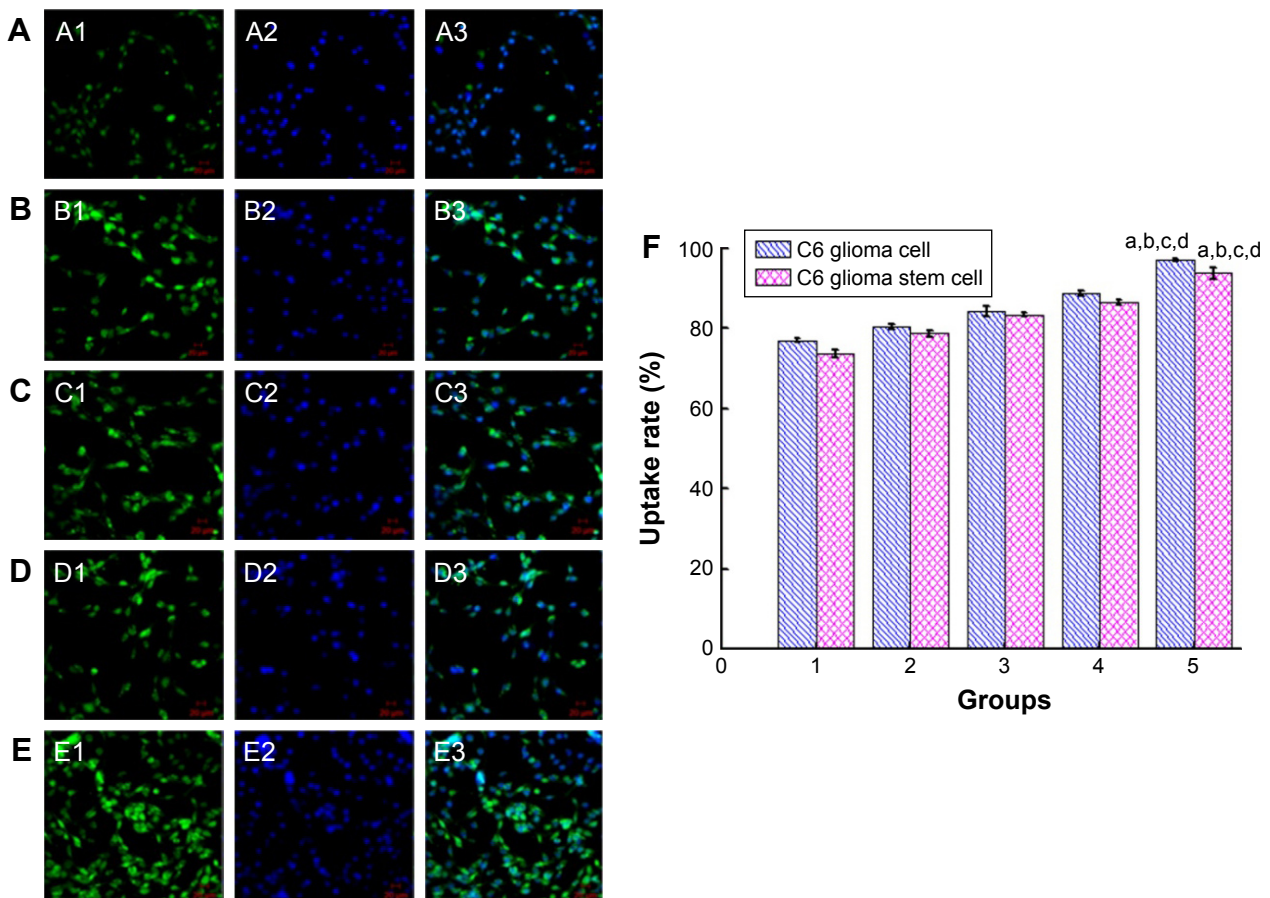
**Figure 5** Cellular uptake and distribution in the GSCs.

**Notes:** Images (**A–E**) represent drug distribution in the C6 GSCs treated with various formulations and detected by laser scanning confocal microscopy. (A1–E1) The green color indicates the drug in the GSCs after applying free curcumin (A1), free curcumin plus quinacrine (B1), curcumin liposomes (C1), curcumin and quinacrine liposomes (D1), and curcumin and quinacrine liposomes modified with MAN (E1), respectively. (A2–E2) The blue color indicates the drug distribution in the C6 GSCs after they were stained with Hoechst 33258. (A3–E3) Overlapping images of A1–A2, B1–B2, C1–C2, D1–D2, and E1–E2. (**F**) The uptake assay of the C6 glioma cells and GSCs. The experimental groups 1, 2, 3, 4, and 5 represent free curcumin, free curcumin plus quinacrine, curcumin liposomes, curcumin and quinacrine liposomes, curcumin and quinacrine liposomes modified with MAN, respectively. [a]$P<0.05$, versus free curcumin; [b]$P<0.05$, versus free curcumin plus quinacrine; [c]$P<0.05$, versus curcumin liposomes; [d]$P<0.05$, versus curcumin and quinacrine liposomes. Magnification ×20.

**Abbreviations:** GSCs, glioma stem cells; MAN, *p*-aminophenyl-α-D-mannopyranoside.
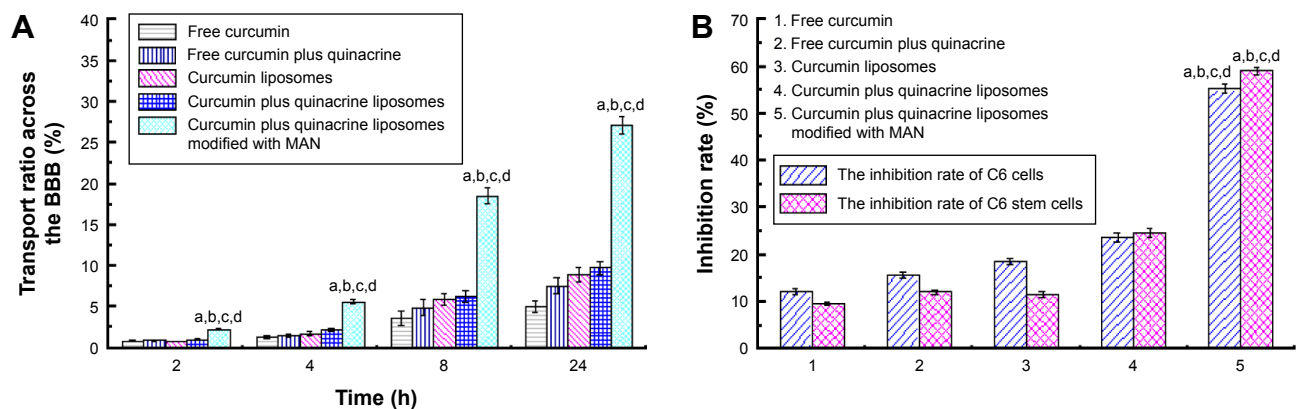


**Figure 6** Eliminating brain glioma along with GSCs in vitro and multifunctional targeting effects in the BBB model.

**Notes:** (**A**) Transport ratios of curcumin across the BBB model in vitro after applying various curcumin formulations. (**B**) Inhibitory ratios of C6 glioma cells and C6 glioma stem cells after they were treated with different curcumin formulations in vitro. Data are presented as the mean ± standard deviation (n=3). [a]$P<0.05$, versus free curcumin; [b]$P<0.05$, versus free curcumin plus quinacrine; [c]$P<0.05$, versus curcumin liposomes; [d]$P<0.05$, versus curcumin and quinacrine liposomes.

**Abbreviations:** BBB, blood–brain barrier; GSCs, glioblastoma stem cells; MAN, *p*-aminophenyl-α-D-mannopyranoside; SD, standard deviation.

curcumin and quinacrine liposomes modified with MAN not only exhibited the strongest transport ability across the BBB, but also showed the strongest inhibitory effect on C6 glioma cells and GSCs in the co-cultured model.

## Evaluation of animal models in vivo

### Survival curves

Figure 7A shows the Kaplan–Meier survival curves of brain glioma-bearing mice, which arose from GSCs. The order of the median survival curve of each group is as follows: curcumin and quinacrine liposomes modified with MAN (34 days) > curcumin and quinacrine liposomes (27 days, $P=0.032$) > curcumin liposomes (25 days, $P=0.029$) > free curcumin and quinacrine (22 days, $P=0.012$) > free curcumin (21 days, $P=0.010$) > physiologic saline (19 days, $P=0.006$). These findings demonstrated that curcumin and quinacrine liposomes group achieved the longest survival

time (15–48 days) compared to the physiological saline group (10–26 days).

### Inhibitory rates of gliomas in animals

The order of the inhibitory rates was: physiologic (0.9%) saline (102%±12.34%) > free curcumin (82.4%±7.95%) > free curcumin and quinacrine (72.59%±8.02%) > curcumin liposomes (58.7%±8.19%) > curcumin and quinacrine liposomes (48.32%±7.54%) > curcumin and quinacrine liposomes modified with MAN (34.65%±9.74%) at day 18 (Figure 7B). These findings signify that the curcumin and quinacrine liposomes modified with MAN attained the most significant difference among the formulations tested.

### HE staining

Regarding the HE staining, Figure 7C1 displays the normal brain tissue. The gliomas infiltrated the brain tissues, but
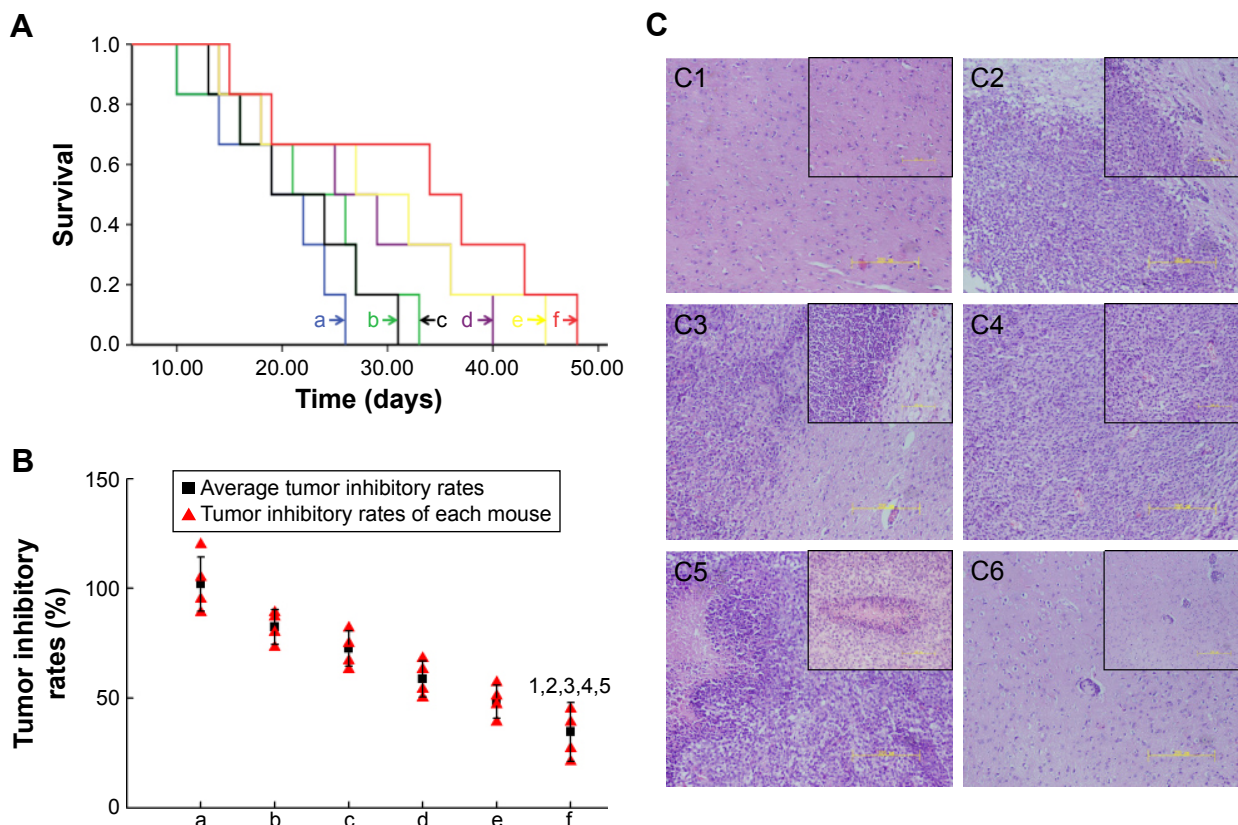


**Figure 7** The inhibitory effects in glioma-bearing imprinting control region mice after treatment with varying formulations.
**Notes:** (**A**) Kaplan–Meier survival curves (n=6 for each group). (**B**) Tumor inhibitory rates of glioma-bearing mice (n=4 for each group): [a]physiologic (0.9%) saline; [b]free curcumin; [c]free curcumin and quinacrine; [d]curcumin liposomes; [e]curcumin and quinacrine liposomes; [f]curcumin and quinacrine liposomes modified with MAN. 1, $P<0.05$, versus physiologic (0.9%) saline; 2, $P<0.05$, versus free curcumin; 3, $P<0.05$, versus free curcumin plus quinacrine; 4, $P<0.05$, versus curcumin liposomes; 5, $P<0.05$, versus curcumin and quinacrine liposomes. (**C**) Images of HE staining: C1, normal brain tissue; C2, the gliomas infiltrated the brain tissues after treatment with physiologic saline; C3, the gliomas were significantly shrunken and generated numerous vacuoles after treatment with curcumin and quinacrine liposomes modified with MAN; C4, the brain gliomas were irregular and lacking an envelope and obvious boundaries after treatment with curcumin and quinacrine liposomes; C5, there were large portions of necrosis and hemorrhage area in the tumor area after treatment with free curcumin and quinacrine; C6, the tumor and tumor clusters at the border of the brain gliomas and normal brain tissues after treatment with free curcumin. The magnification for the non-framed image is ×100. The black-framed image is ×200.
**Abbreviation:** MAN, p-aminophenyl-α-D-mannopyranoside.

the boundary remained visible at the junction with the normal brain tissues (Figure 7C2). Some gliomas continued to rapidly proliferate in the brain section of the curcumin and quinacrine liposomes modified with MAN compared to those in the controlled group. However, the gliomas in the former group were significantly shrunken and generated abnormal gliomas with regions of numerous vacuoles. Some gliomas were retained and some glioma clusters recurred (Figure 7C3). The shape of the brain gliomas was irregular, lacking obvious boundaries. Bleeding and necrotic areas were also noted (Figure 7C4). Large portions of necrosis and hemorrhage were apparent at the largest tumor area. Microvessels full of red blood cells were abundant and were surrounded by the necrotic area (Figure 7C5). The gliomas and glioma clusters, which were mostly oval shaped and were rapidly dividing and proliferating around the blood vessels, were scattered at the border of the brain gliomas and normal brain tissues (Figure 7C6).

## Discussion

The main problem in the chemotherapeutic treatment of brain gliomas lies in the delivery system crossing the BBB and the successful induction of stem cell apoptosis. Hydrophobic drugs and hydrophilic drugs could both be loaded into liposomes. These two kinds of drugs can be loaded into different areas of the liposomes, so that the interactions between drugs could be avoided and the physical stability of drugs increased.

During the process of preparing drug-loaded liposomes, the EE of curcumin was determined by Sephadex-G-50 column chromatography.[33] In the early stages, the curcumin liposomes were easily eluted by PBS, but it was difficult to elute free curcumin due to the former's adsorption on the column. Therefore, the solution had a better solubility with free curcumin which was in need. Theoretically speaking, curcumin can be dissolved in ethanol in accordance with its solubility. The column was consist of dextran, which will shrink if being eluted by ethanol at a concentration of 10%, 20%, 30%, and 40%, respectively. After testing repeatedly for many times, we discovered that free curcumin could be eluted by PBS with 30% ethanol and barely influenced the column efficiency. What is more, in order to observe the influence on EE, different drug–lipid ratios and lipid–CHOL ratios were tested. In this, we found the liposomes' EE increased with increasing amount of lipids. When the lipid–CHOL ratio was 4:1, optimal EE of curcumin could be obtained in the liposomes. However, at this lipid-CHOL ratio, the liposomes appeared to have heavy flocculation. Therefore,

the lipid-CHOL ratio was further optimized to 2:1 in order to make the liposomes more stable.

Electron microscopic technology made it possible to accurately measure the size of prepared liposomes.[34] At the beginning, the size and surface of the liposomes were detected by scanning electron microscopy. However, the liposomes could not be well dispersed into a powder status because of their stickiness after being frozen and dried. Furthermore, the detection of liposomes also was difficult due to the relative magnification of the scanning electron microscope. Given these reasons, we chose to use TEM. After negative staining by 2% phosphotungstic acid and 1% uranyl acetate water separately, we found that the latter could render clearer images of the liposomes. In the process of negative staining, a proper concentration of liposomes was needed while they were captured by the copper screen. That was because the adherent would increase if the liposomes were too thick. Furthermore, excessive coverage may influence the results because of repeated staining. When excess uranyl acetate water remained, the liposomes must be removed after reaction for 1 min and then treated by filter paper.

Three primary methods are currently available for separating and purifying brain GSCs.[35] These approaches include the suspension growth method (single-cell cloning method), CD133 immunomagnetic beads, and SP-cell identification method.[36–38] The CD133-positive cells or the SP cells only reflected a part of the brain GSCs. Meanwhile, the monoclonal C6 GSCs spheroids must be incubated by the suspension growth method. The characteristic markers of stem cell surface expression included CD133 and nestin. CD133 is a kind of transmembrane protein. As a marker of GSCs, CD133 shows strong positive expression and is gradually downregulated till they are totally differentiated. However, researches[39–41] showed that a small group of CD133⁻ expressing glioma cells have the same characteristics as GSCs. The CD133⁺ expressing glioma cells could be selected by flow cytometry or immunomagnetic beads. After that, the rest of the CD133⁻ expressing glioma cells could also aggregate to spheres, and thus, a large number of adherent cells formed. These adherent cells would lose the cloning capacity after being diluted to single ones. Moreover, fewer CD133⁺ expressing glioma cells existed in glioma spheres that were treated with growth factors, compared with highly expressing Nestin⁺ glioma cells. Furthermore, the expression of nestin was also found on CD133⁺ glioma cells under confocal microscopy treated by immunohistochemical staining. So, the C6 stem cells could be identified by flow cytometry after they were treated with nestin.

The main obstacle in brain glioma-targeting research is the BBB, which greatly resists the delivery of numerous drugs to brain tissues. As such, the BBB causes considerable difficulty in the diagnosis and treatment of CNS diseases. According to a report,[42] GLUT1 could help transport drugs across the BBB and finally increase the amount of drugs in the brain because of its high expression on the BBB and brain glioma cells. MAN is able to be specifically binded with GLUT1. Thus, in this research, MAN was bound to the surface of the liposomes as a targeting ligand, which played a major role in assisting the drug-loaded liposomes be delivered across the BBB and enhancing their ability of targeting brain gliomas.

The BBB model in vivo was built using bEnd.3 cells in this research. The TEER resistance value, morphology, and horseradish peroxidase permeability were used to evaluate whether intercellular tight junctions existed among the brain microvascular endothelial cells and assess whether the BBB model in vivo was built successfully. Also, in view of the limitation of BBB and the delivery capability significantly enhanced by curcumin and quinacrine liposomes modified with MAN, we could somehow indicate that MAN could enhance liposome-mediated transportation across the BBB.

In fact, with regard to brain glioma patients being cured, a small part of them recurred after a long time. The possible reason might be the elusive GSCs. Theoretically, if GSCs could be fully eliminated, the brain gliomas were supposed to be eradicated. The cytotoxicity experiment demonstrated the inhibitory effects on C6 glioma cells and C6 GSCs treated with targeted liposomes. The inhibitory effect of curcumin itself was obvious, and it was enhanced when combined with quinacrine. According to this research, curcumin and quinacrine liposomes modified with MAN were able to inhibit C6 glioma cells and C6 GSCs more significantly compared with other control groups. However, the possible reason of this inhibitory effect on GSCs might be related to the Ras/MAPK signaling pathway.[43] In this pathway, more MMP-9 was secreted while transforming growth factor-β was inhibited.[44] Meanwhile, the inhibitory effect might also be relevant to the NF-κB signaling pathway.[45] The proliferation of GSCs was limited when IKK (inhibitor of nuclear factor kappa-B kinase) was inhibited. Furthermore, the results of confocal microscopy experiment and uptake experiment indicated that the targeted liposomes could be taken up by the GSCs very well which would induce their death later. It also implied that quinacrine was capable of promoting tumor apoptosis.

Curcumin could induce GSC apoptosis and the effects could be enhanced by quinacrine, which was capable of inhibiting the expression of Bcl-2 and activating both caspase-9 and downstream caspase-3.[46–48] Previous studies found[49,50] that the inhibitory mechanism of p53 that relied on NF-κB existed in the kidney cancer cells. Quinacrine inhibited NF-κB and activated tumor suppressors of p53 simultaneously. Meanwhile, p53 could effectively activate cell apoptosis by temporarily or permanently blocking cells proliferation.[51] Results showed that curcumin and quinacrine liposomes modified with MAN significantly promoted the apoptosis of C6 glioma cells and C6 GSCs. The reason might be the inhibition of Bcl-2 and activation of caspase-9, caspase-3, and p53. Moreover, Bcl-2 and caspase could also be obviously inhibited by curcumin and quinacrine, inducing the apoptosis of glioma cells and GSCs.

Currently, a major part of the particle delivery system evaluation is focused on its absorption and distribution inside the body.[52] In this experiment, the distribution of curcumin and quinacrine liposomes modified with MAN in the cells was detected by confocal scanning microscopy. Given the results of flow cytometry, we discovered that curcumin and quinacrine liposomes modified with MAN were highly distributed in the nucleus and could be better absorbed by cells, in comparison to other formulations.

ICR mice are well adapted and grow quickly, making the experiments reproducible; therefore, they are generally used in the studies of pharmacology, toxicology, and tumor research, in order to duplicate the animal model.[53,54] Thus, ICR mice were chosen to be the ideal model for this experiment. In this study, C6 GSCs were implanted into mice brain tissues to construct animal models because C6 GSCs showed better proliferative and invasive abilities compared to C6 glioma cells. In the procedure of constructing the animal models, we ensured that C6 GSCs were fully gathered and prolonged the retention time at the inoculating area in order to successfully implant them into animals.

Animal experiments demonstrated that the median survival and inhibitory rates for the curcumin and quinacrine liposomes modified with MAN were obviously higher than those of the other groups. The possible reasons might be as follows. Firstly, DSPE-PEG$_{2000}$ chain could help the targeted liposomes escape to be captured by the endothelial system. Also, MAN was able to improve the transport of targeted liposomes across the BBB and let them work. Apoptosis of GSCs might be induced after the Ras/MAPK signaling pathway was inhibited by curcumin while Bcl-2 was inhibited by quinacrine.[55]

## Conclusion

Curcumin and quinacrine liposomes modified with MAN constructed in the experiment were used to treat brain glioma

cells and brain GSCs. Evaluations of the experiments in vitro revealed that the targeted liposomes could inhibit the growth of glioma cells and GSCs. In the delivery system, quinacrine played an important role in enhancing the apoptosis effects of curcumin on these two kinds of cells. Also, MAN was able to assist the drugs be transported across the BBB, enhancing the drug uptake ability. In vivo experiments had also proved that the targeted liposomes were able to prolong the survival time of glioma-bearing mice and increase the inhibitory rates of gliomas. Generally, the curcumin and quinacrine liposomes modified with MAN provided a potential treatment strategy for the brain glioma cells and brain GSCs.

## Acknowledgments

## Disclosure

The authors report no conflicts of interest in this work.

## References

1. Jagtap JC, Parveen D, Shah RD, et al. Secretory prostate apoptosis response (Par)-4 sensitizes multicellular spheroids (MCS) of glioblastoma multiforme cells to tamoxifen-induced cell death. *FEBS Open Bio*. 2014;5:8–19.
2. Kassis J, Lauffenburger DA, Turner T, Wells A. Tumor invasion as dysregulated cell motility. *Semin Cancer Biol*. 2001;11(2):105–117.
3. Johnson DR, O'Neill BP. Glioblastoma survival in the United States before and during the temozolomide era. *J Neurooncol*. 2012;107(2): 359–364.
4. Abbott NJ, Rönnbäck L, Hansson E. Astrocyte-endothelial interactions at the blood-brain barrier. *Nat Rev Neurosci*. 2006;7(1):41–53.
5. Pardridge WM. CSF, blood-brain barrier, and brain drug delivery. *Expert Opin Drug Deliv*. 2016;13(7):963–975.
6. Peluffo H, Unzueta U, Negro-Demontel ML, et al. BBB-targeting, protein-based nanomedicines for drug and nucleic acid delivery to the CNS. *Biotechnol Adv*. 2015;33(2):277–287.
7. Jhaveri N, Chen TC, Hofman FM. Tumor vasculature and glioma stem cells: contributions to glioma progression. *Cancer Lett*. 2016;380(2): 545–551.
8. Bexell D, Svensson A, Bengzon J. Stem cell-based therapy for malignant glioma. *Cancer Treat Rev*. 2013;39(4):358–365.
9. Chan XH, Nama S, Gopal F, et al. Targeting glioma stem cells by functional inhibition of a prosurvival oncomiR-138 in malignant gliomas. *Cell Rep*. 2012;2(3):591–602.
10. Gangemi R, Paleari L, Orengo AM, et al. Cancer stem cells: a new paradigm for understanding tumor growth and progression and drug resistance. *Curr Med Chem*. 2009;16(14):1688–1703.
11. Huang EH, Heidt DG, Li CW, Simeone DM. Cancer stem cells: a new paradigm for understanding tumor progression and therapeutic resistance. *Surgery*. 2007;141(4):415–419.
12. Scatena R, Bottoni P, Giardina B. Circulating tumour cells and cancer stem cells: a role for proteomics in defining the interrelationships between function, phenotype and differentiation with potential clinical applications. *Biochim Biophys Acta*. 2013;1835(2):129–143.

13. Battelli MG, Musiani S, Monti B, et al. Ricin toxicity to microglial and monocytic cells. *Neurochem Int*. 2001;39(2):83–93.
14. Pardridge WM. Blood-brain barrier biology and methodology. *J Neurovirol*. 1999;5(6):556–569.
15. Yu Y, Clippinger AJ, Pierciey FJ Jr, Alwine JC. Viruses and metabolism: alterations of glucose and glutamine metabolism mediated by human cytomegalovirus. *Adv Virus Res*. 2011;80:49–67.
16. Navone SE, Marfia G, Nava S, et al. Human and mouse brain-derived endothelial cells require high levels of growth factors medium for their isolation, in vitro, maintenance and survival. *Vasc Cell*. 2013;5(1):10.
17. Ying X, Wen H, Lu WL, et al. Dual-targeting daunorubicin liposomes improve the therapeutic efficacy of brain glioma in animals. *J Control Release*. 2010;141(2):183–192.
18. Hao ZF, Cui YX, Li MH, et al. Liposomes modified with p-aminophenyl-α-d-mannopyranoside: a carrier for targeting cerebral functional regions in mice. *Eur J Pharm Biopharm*. 2013;84(3):505–516.
19. Bose S, Panda AK, Mukherjee S, Sa G. Curcumin and tumor immune-editing: resurrecting the immune system. *Cell Div*. 2015;10:6.
20. Saha S, Adhikary A, Bhattacharyya P, Das T, Sa G. Death by design: where curcumin sensitizes drug-resistant tumours. *Anticancer Res*. 2012;32(7):2567–2584.
21. Li Y, Zhang T. Targeting cancer stem cells by curcumin and clinical applications. *Cancer Lett*. 2014;346(2):197–205.
22. Almanaa TN, Geusz ME, Jamasbi RJ. Effects of curcumin on stem-like cells in human esophageal squamous carcinoma cell lines. *BMC Complement Altern Med*. 2012;12:195.
23. Yang LI, Zhang LX, Meng YS. Mitochondrial targeting liposomes incorporating daunorubicin and quinacrine for treatment of relapsed breast cancer arising from cancer stem cells. *Biomaterials*. 2012;33(2): 565–582.
24. Wang W, Ho WC, Dicker DT, et al. Acridine derivatives activate p53 and induce tumor cell death through Bax. *Cancer Biol Ther*. 2005; 4(8):893–898.
25. Friedman J, Nottingham L, Duggal P, et al. Deficient TP53 expression, function, and cisplatin sensitivity are restored by quinacrine in head and neck cancer. *Clin Cancer Res*. 2007;13(1):6568–6578.
26. Guo C, Gasparian AV, Zhuang Z, et al. 9-Aminoacridine-based anticancer drugs target the PI3K/AKT/mTOR, NF-kappaB and p53 pathways. *Oncogene*. 2009;28(8):1151–1161.
27. Sarkar S, Das N. Mannosylated liposomal flavonoid in combating age-related ischemia–reperfusion induced oxidative damage in rat brain. *Mech Ageing Dev*. 2006;127(4):391–397.
28. Xiang Y, Liang L, Wang X, Wang J, Zhang X, Zhang Q. Chloride channel-mediated brain glioma targeting of chlorotoxin-modified doxorubicine-loaded liposomes. *J Control Release*. 2011;152(3):402–410.
29. Li XY, Zhao Y, Sun MG, et al. Multifunctional liposomes loaded with paclitaxel and artemether for treatment of invasive brain glioma. *Biomaterials*. 2014;35(21):5591–5604.
30. Li L, Geisler I, Chmielewski J, Cheng JX. Cationic amphiphilic polyproline helix P11LRR targets intracellular mitochondria. *J Control Release*. 2010;142(2):259–266.
31. Cecchelli R, Dehouck B, Descamps L, et al. In vitro model for evaluating drugtransport across the blood-brain barrier. *Adv Drug Deliv Rev*. 1999;36(2–3):165–178.
32. Li XT, Ju RJ, Li XY, et al. Multifunctional targeting daunorubicin plus quinacrine liposomes, modified by wheat germ agglutinin and tamoxifen, for treating brain glioma and glioma stem cells. *Oncotarget*. 2014;5(15):6497–6511.
33. Zhang L, Qi Z, Xin W, et al. Drug-in-cyclodextrin-in-liposomes: a novel drug delivery system for flurbiprofen. *Int J Pharm*. 2015;492(1–2):40–45.
34. Qiu D, An X, Chen Z, Ma X. Microstructure study of liposomes decorated by hydrophobic magnetic nanoparticles. *Chem Phys Lipids*. 2012;165(5):563–570.
35. Liu J, Qu CB, Xue YX, Li Z, Wang P, Liu YH. MiR-143 enhances the antitumor activity of shikonin by targeting bag3 expression in human glioblastoma stem cells. *Biochem Biophys Res Commun*. 2015; 468(1–2):105–112.

36. Salabi F, Nazari M, Cao WG. Cell culture, sex determination and single cell cloning of ovine, transgenic satellite cells in vitro. *J Biol Res (Thessalon)*. 2014;21(1):22.

37. Zhou X, Zheng C, Shi Q, Li X, Shen Z, Yu R. Isolation, cultivation and identification of brain glioma stem cells by magnetic bead sorting. *Neural Regen Res*. 2012;7(13):985–992.

38. Islam F, Gopalan V, Wahab R, Smith RA, Lam KY. Cancer stem cells in oesophageal squamous cell carcinoma: identification, prognostic and treatment perspectives. *Crit Rev Oncol Hematol*. 2015;96(1):9–19.

39. Beier D, Hau P, Proescholdt M, et al. CD133(+) and CD133(−) glioblastoma-derived cancer stem cells show differential growth characteristics and molecular profiles. *Cancer Res*. 2007;67(9):4010–4015.

40. Wang J, Sakariassen PØ, Tsinkalovsky O, et al. CD133 negative glioma cells form tumors in nude rats and give rise to CD133 positive cells. *Int J Cancer*. 2008;122(4):761–768.

41. Joo KM, Kim SY, Jin X, et al. Clinical and biological implications of CD133-positive and CD133-negative cells in glioblastomas. *Lab Invest*. 2008;88(8):808–815.

42. Gorin F, Harley W, Schnier J, Lyeth B, Jue T. Perinecrotic glioma proliferation and metabolic profile within an intracerebral tumor xenograft. *Acta Neuropathol*. 2004;107(3):235–244.

43. Santibáñez JF, Guerrero J, Quintanilla M, Fabra A, Martínez J. Transforming growth factor-β1 modulates matrix metalloproteinase-9 production through the Ras/MAPK signaling pathway in transformed keratinocytes. *Biochem Biophys Res Commun*. 2002;296(2):267–273.

44. Tyagi N, Dash D, Singh R. Curcumin inhibits paraquat induced lung inflammation and fibrosis by extracellular matrix modifications in mouse model. *Inflammopharmacology*. 2016;24(6):335–345.

45. Sahin K, Pala R, Tuzcu M, et al. Curcumin prevents muscle damage by regulating NF-κB and Nrf2 pathways and improves performance: an in vivo model. *J Inflamm Res*. 2016;9:147–154.

46. Du WZ, Feng Y, Wang XF, et al. Curcumin suppresses malignant glioma cells growth and induces apoptosis by inhibition of SHH/GLI1 signaling pathway in vitro and vivo. *CNS Neurosci Ther*. 2013;19(12):926–936.

47. Huang TY, Tsai TH, Hsu CW, Hsu YC. Curcuminoids suppress the growth and induce apoptosis through caspase-3-dependent pathways in glioblastoma multiforme (GBM) 8401 cells. *J Agric Food Chem*. 2010;58(19):10639–10645.

48. Zanotto-Filho A, Braganhol E, Edelweiss MI, et al. The curry spice curcumin selectively inhibits cancer cells growth in vitro, and in preclinical model of glioblastoma. *J Nutr Biochem*. 2012;23(6):591–601.

49. Geng Y, Kohli L, Klocke BJ, Roth KA. Chloroquine-induced autophagic vacuole accumulation and cell death in glioma cells is p53 independent. *Neuro Oncol*. 2010;12(5):473–481.

50. Dermawan JK, Gurova K, Pink J, et al. Quinacrine overcomes resistance to erlotinib by inhibiting FACT, NF-κB, and cell-cycle progression in non-small cell lung cancer. *Mol Cancer Ther*. 2014;13(9):2203–2214.

51. Mohapatra P, Preet R, Das D, et al. Quinacrine-mediated autophagy and apoptosis in colon cancer cells is through a p53-and p21-dependent mechanism. *Oncol Res*. 2012;20(2–3):81–91.

52. Ghaffari A, Manafi A, Moghimi HR. Clindamycin phosphate absorption from nanoliposomal formulations through third-degree burn eschar. *World J Plast Surg*. 2015;4(2):145–152.

53. Kim J, Ekram MB, Kim H, et al. Imprinting control region (ICR) of the Peg3 domain. *Hum Mol Genet*. 2012;21(12):2677–2687.

54. Li XY, Zhao Y, Sun MG, et al. Multifunctional liposomes loaded with paclitaxel and artemether for treatment of invasive brain glioma. *Biomaterials*. 2014;35(21):5591–5604.

55. Changchien JJ, Chen YJ, Huang CH, et al. Quinacrine induces apoptosis in human leukemia K562 cells via p38 MAPK-elicited BCL2 down-regulation and suppression of ERK/c-Jun-mediated BCL2L1 expression. *Toxicol Appl Pharmacol*. 2015;284(1):33–41.